Tunnelling and Underground Space Technology 43 (2014) 133–139

Contents lists available at ScienceDirect

Tunnelling and Underground Space Technology

journal homepage: www.elsevier.com/locate/tust

Analysis of the influence of range and angle of incidence of terrestrial laser scanning measurements on tunnel inspection

Javier Roca-Pardiñas [a], Ramón Argüelles-Fraga [b], Francisco de Asís López [b], Celestino Ordóñez [b,*]

[a] *Department of Statistics, University of Vigo, Campus Lagoas-Marcosende, 36310 Vigo, Pontevedra, Spain*
[b] *Department of Mining Exploitation and Prospecting, Polytechnic School of Mieres, University of Oviedo, Campus de Mieres, C/Gonzalo Gutiérrez, s/n, 33600 Mieres, Spain*

ARTICLE INFO

Article history:
Received 24 September 2013
Received in revised form 24 April 2014
Accepted 28 April 2014
Available online 27 May 2014

Keywords:
Terrestrial laser scanner
Monte Carlo simulation
Measurement geometry
Tunnel inspection
Nonparametric regression

ABSTRACT

Terrestrial Laser Scanner (TLS) measurements are subject to errors which influence the quality of the 3D models built from the point clouds. In this paper, a methodology to build an error model of the TLS measurements is proposed. Measurement errors are estimated based on two of the factors that mostly affect their magnitude: distance to the object and angle of incidence.

The error model is used to analyze, by means of Monte Carlo simulation, the spatial distribution of the errors in a point cloud of a circular tunnel section and also to simulate the effect of the measurement error in tunnel inspection works.

The results obtained indicate that although the angle of incidence influences the point cloud quality when the laser is located near the tunnel gable, its effect is counteracted by the point density when a surface is fitted to the point cloud.

© 2014 Elsevier Ltd. All rights reserved.

1. Introduction

In the last few years, Terrestrial Laser Scanners (TLS) have become systems frequently used in inverse engineering and in the quality control of facilities and infrastructures (Armesto et al., 2008; Armesto et al., 2009; Gordon and Lichti, 2007; Tang et al., 2010; Teza and Pesci, 2012; Von Der Haar et al., 2013).

Regarding tunnels, the use of TLS has become popular in recent years with various applications such as geotechnical studies (Fekete and Diederichs, 2013; Fekete et al., 2009, 2010), deformation analysis (Gosliga et al., 2006; Lam, 2006; Qiu et al., 2009; Wang et al., 2009) and inspection (Pejić, 2013; Sandrone and Wissler, 2012).

The accuracy of the point cloud obtained with these systems depends on different factors: distance to the object, angle of incidence, material of the measured object, environmental conditions, etc. (Kaasalainen et al., 2011; Lee et al., 2010; Pesci et al., 2011; Yang et al., 2011; Zhu et al., 2008). For properly calibrated equipment, working on suitable environmental conditions and measuring on homogeneous material, the distance to the object, and especially the angle of incidence of the laser beam with the object surface, determine the spatial distribution of the errors in the point cloud (Argüelles-Fraga et al., 2013; Pejić, 2013; Soudarissanane et al., 2011). These errors increase with range and angle of incidence. However, when performing quality control works aimed at establishing whether the surface of an object (bridge, tunnel, industrial part, etc.) matches the theoretical surface (Golparvar-Fard et al., 2011; Guarnieri et al., 2013; Monserrat and Crosetto, 2008), we tend to consider that the point cloud obtained with TLS systems is error free or, to a lesser extent, that errors correspond to their nominal value given by the manufacturer. This assumption may lead to erroneous conclusions about the quality of the measured objects, which may have, in turn, a negative economic impact.

Since there is no standardized procedure such as the DIN 18723 or the ISO 17123, which apply to total stations, it is necessary to develop models for TLS measurement errors if we aim to have an estimation of the quality of the 3D models built from the point clouds.

In this paper, we propose the development of an error model based on empirical results in order to study the distribution of the errors through the scanned surface. Then, this model is used to establish conclusions about the effect of the angle of incidence, the distance to the object and the position of the scanner, in tunnel inspection.

2. Error model

In this work, an error model based on experimental data was constructed. First, we assume that each laser point $P_i^{\bullet} = (X_i^{\bullet}, Y_i^{\bullet}, Z_i^{\bullet})$

* Corresponding author. Tel.: +34 985 458 027; fax: +34 985 458 001.
E-mail addresses: roca@uvigo.es (J. Roca-Pardiñas), mon@uniovi.es (R. Argüelles-Fraga), franasisloal@gmail.com (F. de Asís López), ordonezcelestino@uniovi.es (C. Ordóñez).

http://dx.doi.org/10.1016/j.tust.2014.04.011
0886-7798/© 2014 Elsevier Ltd. All rights reserved.

of the point cloud, for $i = 1, \ldots, n$, is a measure of the theoretical point on the scanned object plus a term of error ε_i:

$$(X_i^{\bullet}, Y_i^{\bullet}, Z_i^{\bullet}) = (X_i, Y_i, Z_i) + \varepsilon_i \tag{1}$$

As we have no information concerning the spatial distribution of $\varepsilon_i = (\varepsilon_{X_i}, \varepsilon_{Y_i}, \varepsilon_{Z_i})$, and assuming that its components are independent, it was considered, for simplicity, that the error is spatially distributed on a spherical surface whose radius R_i is considered as a Gaussian random variable with mean μ_i and standard deviation σ_i: $R_i \in N(\mu_i, \sigma_i)$.

At this point, our interest relies on establishing a model relating the measurement error R_i with the scanning range r_i and the angle of incidence α_i of the laser beam on the object surface. In fact, we are interested in determining two functions f and g, where f represents the average measurement error (the mean radius of the sphere) and g the dispersion of that error, as follows:

$$\mu_i = f(r_i, \alpha_i) \text{ and } \sigma_i = g(r_i, \alpha_i) \tag{2}$$

For this purpose, an experiment was carried out, consisting in scanning a flat panel placed at different distances and incident angles with respect to a laser scanner. Specifically, the following ranges and incidence angles were considered:

- Range (m): 12.5, 25, 37.5, 50, 62.5, 75, 87.5, 100, 112.5, 125, 137.5 and 150.
- Angle of incidence (degrees): 0, 10, 20, 30, 40, 50, 60, 70 and 80.

All the different combinations between angles and ranges were tested, resulting in a total of 108 different point clouds. For each point cloud, a plane was fitted by means of a Principal Component Analysis (PCA). In particular, the fitted plane is determined by the third principal component of the PCA. Accordingly, the weighted sample covariance matrix in any point (x_0, y_0) in the XY plane is calculated:

$$\Sigma(x_0, y_0) = \begin{pmatrix} \sigma_X^2 & \sigma_{XY} & \sigma_{XZ} \\ \sigma_{XY} & \sigma_Y^2 & \sigma_{YZ} \\ \sigma_{XZ} & \sigma_{YZ} & \sigma_X^2 \end{pmatrix} = \frac{1}{\sum_{i=1}^{n} W_i} \sum_{i=1}^{n} (P_i^{\bullet} - \bar{P}^{\bullet}) W_i (P_i^{\bullet} - \bar{P}^{\bullet})^T \tag{3}$$

Being n the number of points in each point cloud and W_i a weight function. For this particular case, where the surface fitted to the point cloud is a plane, the weighted function was considered the identity matrix.

Then, the eigenvalues of the covariance matrix are calculated according to Eq. (3). In general, the smallest eigenvalue corresponds to the normal of the best-fitted plane

$$\hat{a}(x - \overline{X^{\bullet}}) + \hat{b}(y - \overline{Y^{\bullet}}) + \hat{c}(z - \overline{Z^{\bullet}}) = 0 \tag{4}$$

Once the plane was obtained, the following procedure was carried out in order to obtain an estimation of R_i depending on the distance to the object and the angle of incidence:

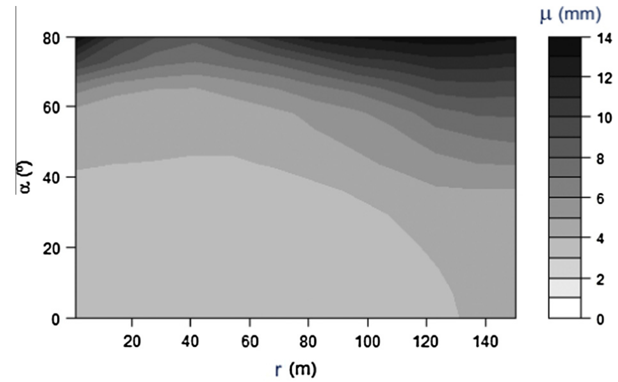

Fig. 2. Estimated raster surface $\hat{f}(r, \alpha)$ as a function of the distance to the object r (in meters) and the angle of incidence α (in degrees). Each pixel in the image represents a value of the mean error in mm.

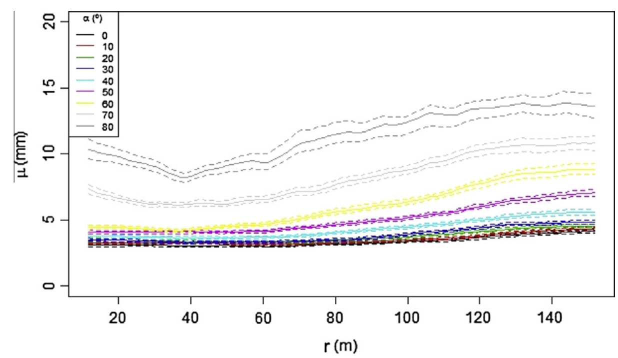

Fig. 3. Estimated function $\hat{f}_1(r) = \hat{f}(r, \alpha)$, and the corresponding 95% simulation interval, as a function of the distance to the object.

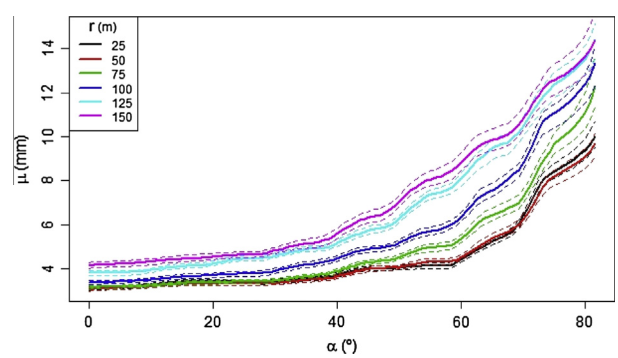

Fig. 4. Estimated curve $\hat{f}_2(\alpha) = \hat{f}(r, \alpha)$, and the corresponding 95% simulation interval, as a function of the angle of incidence.

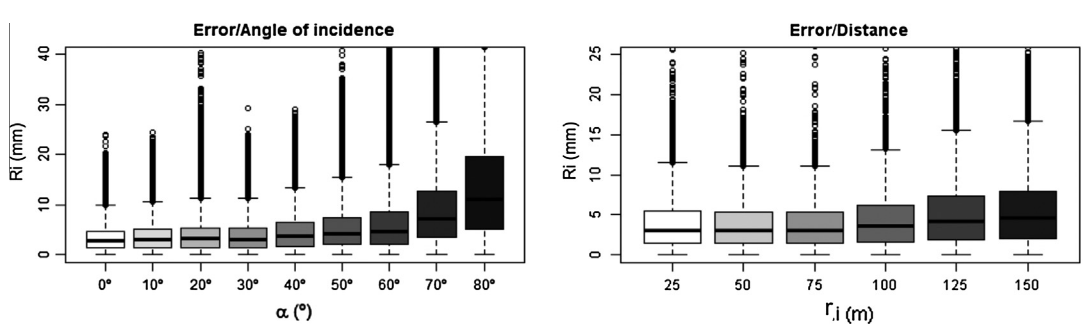

Fig. 1. Boxplot of the measurement error (R_i) depending on the angle of incidence (left) and the distance to the object (right).

Download English Version:

https://daneshyari.com/en/article/311840

Download Persian Version:

https://daneshyari.com/article/311840

Daneshyari.com